Functional Materials

Highly Interpenetrated Metal–Organic Frameworks for Hydrogen Storage**

*Banu Kesanli, Yong Cui, Milton R. Smith, Edward W. Bittner, Bradley C. Bockrath, and Wenbin Lin**

Metal–organic frameworks (MOFs) provide an interesting avenue to novel materials through fine-tuning their structures by a modular construction approach.[1] A variety of MOFs have recently been explored for potential applications, such as nonlinear optics, size-, shape-, and functional-group-selective sorptions, and catalysis.[2] Many of the perceived applications for MOFs require accessible large pores, which presents a significant challenge owing to a strong tendency of interpenetration in such very open frameworks. In contrast to a vast number of porous non-interpenetrated MOFs, only a few examples of porous interpenetrated MOFs have been reported.[3]

Kitagawa et al. have pioneered the studies on the adsorption of small molecules (such as methane and oxygen) by microporous MOFs.[4] More recent results by Rosi et al. further suggested that microporous MOFs are able to store hydrogen at a capacity unmatched by other materials.[5] It was believed that favorable interactions exist between aromatic rings of MOFs and hydrogen molecules.[6] We hypothesize that microporous interpenetrated MOFs would be ideal candidates for the sorption of small gaseous molecules. Interpenetration can be utilized to strengthen the interaction between the gaseous molecule and the framework by an entrapment mechanism in which a hydrogen molecule is in close proximity with several aromatic rings from interpenetrating networks.[7] Herein we report the design of highly interpenetrated aromatic-rich MOFs and preliminary data on their hydrogen and methane sorption capacities.

New aromatic-rich, dicarboxylic acids 6,6′-dichloro-2,2′-diethoxy-1,1′-binaphthyl-4,4′-dibenzoic acid (L_1-H_2) and 6,6′-dichloro-2,2′-dibenzyloxy-1,1′-binaphthyl-4,4′-dibenzoic acid (L_2-H_2) were prepared by Suzuki coupling reactions between

[*] Dr. B. Kesanli, Dr. Y. Cui, Prof. W. Lin
Department of Chemistry, CB#3290
University of North Carolina
Chapel Hill, NC 27599 (USA)
Fax: (+1) 919-962-2388
E-mail: wlin@unc.edu

Dr. M. R. Smith, Dr. E. W. Bittner, Dr. B. C. Bockrath
National Energy Technology Laboratory
United States Department of Energy
P.O. Box 10940, Pittsburgh, PA 15236 (USA)

[**] We acknowledge financial support from NSF. W.L. is an Alfred P. Sloan Fellow, an Arnold and Mabel Beckman Young Investigator, a Cottrell Scholar of Research Corp, and a Camille Dreyfus Teacher-Scholar. We thank Dr. C. Wu for help with X-ray structure determinations.

Supporting information for this article is available on the WWW under http://www.angewandte.org or from the author.

  DOI: 10.1002/ange.200461214

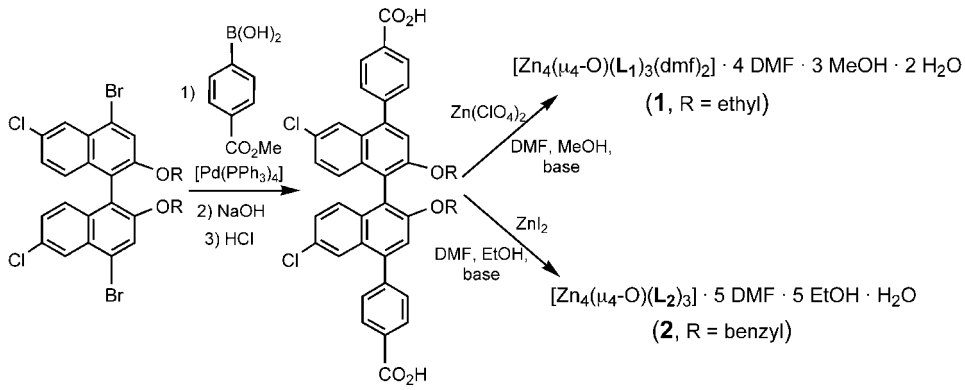

Scheme 1.

4-methoxycarbonylphenylboronic acid and previously reported 6,6′-dichloro-4,4′-dibromo-1,1′-binaphthyl starting materials followed by hydrolysis (Scheme 1).[8] Single crystals of $[Zn_4(\mu_4\text{-}O)(L_1)_3(dmf)_2]\cdot 4\,DMF\cdot 3\,CH_3OH\cdot 2\,H_2O$ (**1**) and $[Zn_4(\mu_4\text{-}O)(L_2)_3]\cdot 5\,DMF\cdot 5\,C_2H_5OH\cdot H_2O$ (**2**) were obtained by treating $Zn(ClO_4)_2$ with L_1-H_2 in DMF and MeOH or ZnI_2 with L_2-H_2 in DMF and EtOH in the presence of dimethylaniline at 50 °C for two days. The formulations of **1** and **2** were supported by IR, microanalysis, and thermogravimetric analysis (TGA) results.

Compound **1** adopts a 3D interpenetrating network structure that is built from two distinct $[Zn_4(\mu_4\text{-}O)(L_1)_3(dmf)_2]$ clusters (Figure 1a).[9] While one of the L_1 ligands adopts an *exo*-tridentate coordination mode, the other L_1 ligands adopt *exo*-tetradentate coordination mode. One of the two $[Zn_4(\mu_4\text{-}O)(L_1)_3(dmf)_2]$ clusters contains three Zn^{II} centers in tetrahedral and one in a trigonal bipyramidal coordination geometry that are bridged by a μ_4-O atom and five carboxylate groups of L_1 ligands, while the other contains three Zn^{II} centers in tetrahedral and one in an octahedral coordination geometry that are bridged by a μ_4-O atom and six carboxylate groups of L_1 ligands. Each of the two $[Zn_4(\mu_4\text{-}O)(L_1)_6(dmf)_2]$ clusters is completed by the coordination of two DMF molecules. Each type of $[Zn_4(\mu_4\text{-}O)(L_1)_6(dmf)_2]$ cluster in **1** is interlinked by the carboxylate groups of L_1 ligands to generate an extended neutral 3D network of a cubic topology that is built upon six-connected nodes. The 3D network of **1** thus possesses very large cubic cavities of approximately $19\times19\times19$ Å (Figure 1b). However, **1** avoids extremely large void space by forming a fourfold interpenetrated structure (Figure 1c). Even after fourfold interpenetration, **1** still possesses significant void space that is occupied by disordered DMF, MeOH, and H_2O guest molecules.[10] These void spaces can be accessed from open channels (Figure 1d) of approximately 4.1×5.0 Å along the *a* axis, of 3.2×4.0 Å and 2×2.5 Å along the *b* axis, and of 4.7×5.4 Å and 1.8×3.4 Å along the *c* axis. The effective free volume of **1** was calculated by PLATON analysis as 46.1% of the crystal volume (15168 $Å^3$ out of the 32912 $Å^3$ unit cell volume).

Compound **2** adopts a similar fourfold 3D interpenetrating network structure that is built from C_3-symmetric $[Zn_4(\mu_4\text{-}O)(L_2)_3]$ clusters.[9] All the Zn centers in the $[Zn_4(\mu_4\text{-}O)(L_2)_3]$ cluster have tetrahedral geometry through coordination to a

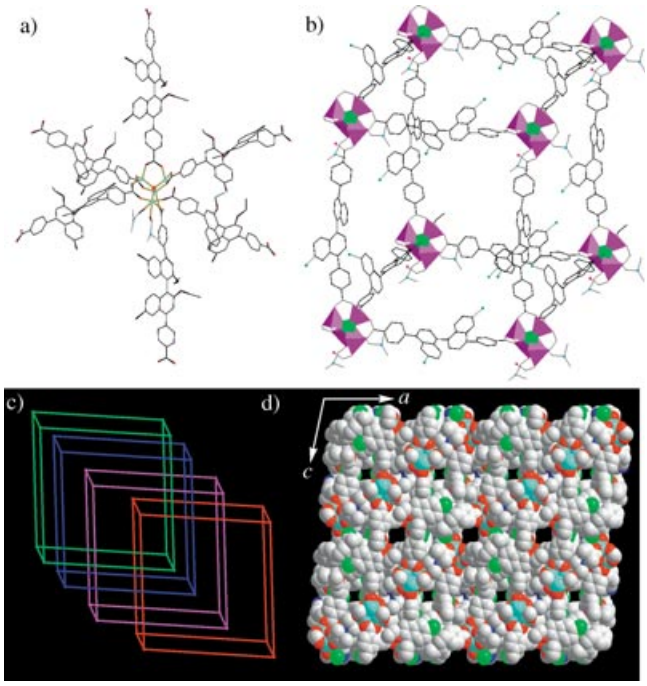

Figure 1. a) A view of the one of the $[Zn_4(\mu_4\text{-}O)(L_1)_6(dmf)_2]$ clusters of **1** b) A view of the cubic cavity formed by the 3D network (ethoxy groups have been omitted for clarity; the purple and green polyhedra represent the cluster building unit. c) A schematic presentation of the fourfold interpenetration in **1**. d) A space-filling model of **1** as viewed down the *b* axis (solvent molecules have been omitted); gray C, red O, blue N, green Cl, turquoise Zn.

μ_4-oxygen atom and three oxygen atoms of the bridging carboxylate groups of the L_2 ligands. There are no coordinating solvent molecules in the structure of **2**. Just like **1**, the $[Zn_4(\mu_4\text{-}O)(L_2)_3]$ clusters in **2** are linked by L_2 ligands to form an extended 3D network structure of a cubic topology. The 3D network structure of **2** contains cubic cavities of approximately $19\times19\times19$ Å. The porosity of **2** is drastically reduced by adopting fourfold interpenetration, and the void space in **2** is filled with five DMF, one H_2O, and five ethanol guest molecules as established by TGA and elemental analysis. PLATON analysis indicated that the effective free volume of **2** was 41.4% of the crystal volume (5257 $Å^3$ out of the

12699 Å^3 unit cell volume). A smaller percent effective free volume of **2** compared to **1** is consistent with the presence of larger benzyloxy groups in **2**. The void space of **2** is only accessible along the *c* axis by open channels of approximately 1.3×4.5 Å.

Single-crystal X-ray diffraction studies, TGA, and elemental analyses demonstrated the inclusion of disordered guest molecules in **1** and **2**. Powder X-ray diffraction studies further indicated that the long-range order of the framework structures of **1** and **2** was retained upon complete removal of the guest molecules (see Supporting Information). Permanent microporosity of **1** and **2** was unambiguously established with CO_2 adsorption measurements at 0 °C. Samples of **1** and **2** were soaked in CH_2Cl_2 overnight and then evacuated at 85 °C for 12 h before CO_2 adsorption measurements. Type 1 behavior was observed for the CO_2 adsorption isotherms of both **1** and **2**, which is characteristic of solids with micropores. Compounds **1** and **2** possess a BET surface area of 502 and 396 $m^2 g^{-1}$, respectively. The micropore volume for **1** is 0.20 $mL g^{-1}$ and for **2** is 0.13 $mL g^{-1}$.[11] Smaller surface area observed for **2** is consistent with its percent effective free volume calculated with PLATON.

We have examined gas storage behaviors of **1** and **2** at room temperature. Hydrogen adsorption isotherms were taken using a pulse mass analyzer[12] in the 0.9–48 bar pressure range on samples of **1** and **2** that had been heated at 150 °C for 1 h to remove the included solvent molecules. The H_2 uptakes are calculated to be 1.12 wt % for **1** and 0.98 wt % for **2** at 48 bar (Figure 2, Table 1), which corresponds to H_2 storage capacity of 124.7 $mL g^{-1}$ for **1** and 109.6 $mL g^{-1}$ for **2**.[12] The H_2 uptake of **1** and **2** is reversible for at least six times. For comparison, MOF-5 reported by Rosi et al.[5] exhibits a H_2 uptake of 1.65 wt % ($\approx$1.5 times that of **1**) using our procedures under the same conditions. These hydrogen uptake results for **1** and **2** are comparable to H_2 storage capacities of purified single-walled carbon nanotubes and only slightly inferior to the best MOFs (which have surface areas of 5–10 times those of **1** and **2**).[5,12,13] Methane-adsorption measurements indicated a room-temperature methane uptake of 11.0 wt % (154 $mL g^{-1}$) for **1** and 9.5 wt % (133 $mL g^{-1}$) for **2**. These methane storage capacities are lower than those of the best MOFs, which is consistent with the smaller microporous surface areas of **1** and **2**.

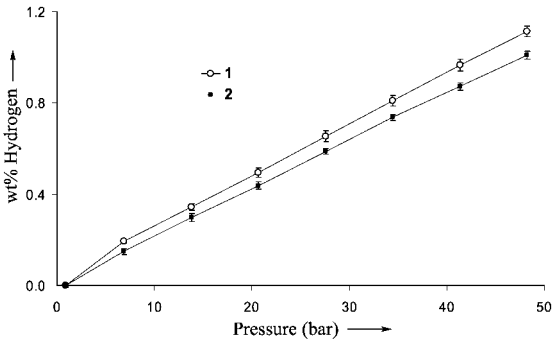

Figure 2. Hydrogen adsorption isotherms of **1** and **2** at 25 °C. The data points represent averages of six consecutive runs and the error bars indicate run-to-run variations.

Table 1: Porosity and gas storage capacity of **1** and **2**.

Sample	Surface area $m^2 g^{-1}$[a]	Pore volume $mL g^{-1}$[b]	Void volume %[c]	wt % H_2	wt % CH_4
1	502	0.20	46.1	1.12	11.0
2	396	0.13	41.4	0.98	9.5

[a] Determined from fits of adsorption data to the BET equation. [b] Calculated using the DR equation. [c] Estimated from PLATON calculations

Our results agree with an earlier observation that large surface area and pore volume are not the only recipe for the attainment of H_2 storage materials.[13a] That significant H_2 uptake is detected in the highly interpenetrated networks of **1** and **2** points to new directions for the design of efficient H_2 storage materials by utilizing interpenetration to strengthen the interaction between H_2 molecules and the framework by multiple contacts with several aromatic rings from the interpenetrating networks. Similar to triple-junction sites in carbon nanotube bundles,[6] such storage sites would have higher H_2 binding energy which is another key to the development of practical H_2 storage materials.

In summary, we have synthesized and characterized two novel fourfold interpenetrated MOFs of cubic topology that exhibit significant H_2 uptake at 25 °C. The ready tunability of these MOFs should allow the optimization of both H_2 storage capacity and H_2 binding energy in future generations of MOFs.

Experimental Section

1: A mixture of $Zn(ClO_4)_2 \cdot 6H_2O$ (3.7 mg, 0.01 mmol) and L_1-H_2 (0.01 mmol) was placed in a small vial containing DMF (0.5 mL), MeOH (0.2 mL), and *N*,*N*′-dimethylaniline (5 μL). The vial was sealed, heated at 50 °C for 48 h, and allowed to cool to room temperature. The crystals suitable for X-ray diffraction were collected by filtration, washed with diethyl ether, and dried in air. Yield: 81 %. Elemental analysis calcd (%) for $C_{135}H_{136}Cl_6Zn_4N_6O_{30}$, C 57.97, H 4.86, N 3.00; found: C 57.96, H 4.85, N 3.79, IR: $\tilde{\nu}$ = 3487 (m), 2978 (w), 2924 (w), 1660 (m), 1603 (s), 1552 (m), 1508 (m), 1411 (s), 1373 (m), 1343 (s), 1324 (m), 1213 (w), 1189 (w), 1155 (w), 1088 (m), 1059 (w), 1019 (m), 948 (w), 866 (w), 816 (w), 788 (w), 723 (w), 699 (w), 625 cm^{-1} (w).

Carbon dioxide adsorption studies were carried out at 0 °C on a Quantachrome-1C surface-area analyzer. Details of hydrogen adsorption studies were described in ref. [12].

Received: July 6, 2004
Revised: August 12, 2004

Keywords: coordination networks · crystal engineering · functional materials · hydrogen storage · zinc

[1] a) B. Moulton, M. Zaworotko, *Chem. Rev.* **2001**, *101*, 1629–1658; b) M. Eddaoudi, D. B. Moler, H. Li, B. Chen, T. M. Reineke, M. O'Keeffe, O. M. Yaghi, *Acc. Chem. Res.* **2001**, *34*, 319–330; c) N. G. Pschirer, D. M. Ciurtin, M. D. Smith, U. H. F. Bunz, H. C. zur Loye, *Angew. Chem.* **2002**, *114*, 603–605; *Angew. Chem. Int. Ed.* **2002**, *41*, 583–585.

[2] a) O. R. Evans, W. Lin, *Acc. Chem. Res.* **2002**, *35*, 511–522; b) B. Kesanli, W. Lin, *Coord. Chem. Rev.* **2003**, *246*, 305–326.

[3] a) T. M. Reineke, M. Eddaoudi, D. Moler, M. O'Keeffe, O. M. Yaghi, *J. Am. Chem. Soc.* **2000**, *122*, 4843 – 4844; b) O. R. Evans, Z. Wang, R.-G. Xiong, B. M. Foxman, W. Lin, *Inorg. Chem.* **1999**, *38*, 2969 – 2973.
[4] a) S. Kitagawa, R. Kitaura, S.-i. Noro, *Angew. Chem.* **2004**, *116*, 2388 – 2430; *Angew. Chem. Int. Ed.* **2004**, *43*, 2334 – 2375; b) S. i. Noro, S. Kitagawa, M. Kondo, K. Seki, *Angew. Chem.* **2000**, *112*, 2161 – 2164; *Angew. Chem. Int. Ed.* **2000**, *39*, 2081 – 2084.
[5] N. L. Rosi, J. Eckert, M. Eddaoudi, D. T. Vodak, J. Kim, M. O'Keeffe, O. M. Yaghi, *Science* **2003**, *300*, 1127 – 1129.
[6] Y. S. Nechaev, O. K. Alexeeva, *Int. J. Hydrogen Energy* **2003**, *28*, 1433 – 1443.
[7] J. Li, T. Furuta, H. Goto, T. Ohashi, Y. Fujiwara, S. Yip, *J. Chem. Phys.* **2003**, *119*, 2376 – 2385.
[8] Y. Cui, O. R. Evans, H. L. Ngo, P. S. White, W. Lin, *Angew. Chem.* **2002**, *114*, 1207 – 1210; *Angew. Chem. Int. Ed.* **2002**, *41*, 1159 – 1162.
[9] X-ray single-crystal diffraction data for both **1** and **2** were collected on a Siemens SMART CCD diffractometer. Crystal data for **1**: monoclinic, space group *C*2, with $a = 32.768(7)$, $b = 39.312(8)$, $c = 25.680(5)$ Å, $b = 95.79(3)°$, $V = 32\,912(11)$ Å^3, $Z = 8$, $\rho_{calcd} = 1.13$ g cm^{-3}. Least-squares refinement based on 21 943 reflections with $I > 2\sigma(I)$ and 1358 parameters led to convergence, with a final $R1 = 0.131$, $R_w2 = 0.373$, and GOF = 1.38. Flack parameter = 0.17(2). Crystal data for **2**: trigonal, space group *R*3, with $a = 36.649(1)$, $c = 10.918(1)$ Å, $V = 12\,699.1(8)$ Å^3, $Z = 3$, $\rho_{calcd} = 1.24$ g cm^{-3}. Least-squares refinement based on 3671 reflections with $I > 2\sigma(I)$ and 163 parameters led to convergence, with a final $R1 = 0.125$, $R_w2 = 0.308$, and GOF = 1.38. The crystal of **2** is refined as a twin structure. CCDC-243787 (**1**) and CCDC-243788 (**2**) contain the supplementary crystallographic data for this paper. These data can be obtained free of charge via www.ccdc.cam.ac.uk/conts/retrieving.html (or from the Cambridge Crystallographic Data Centre, 12 Union Road, Cambridge CB2 1EZ, UK; fax: (+44) 1223-336-033; or deposit@ccdc.cam.ac.uk).
[10] Although the exact locations of the included solvent molecules cannot be unambiguously determined from single crystal X-ray diffraction studies owing to their highly disordered nature, we have resorted to TGA and elemental analyses to establish the formulations of **1** and **2**.
[11] The micropore volume was calculated by fitting the adsorption data to the Dubinin–Radushkevich (DR) equation.
[12] M. R. Smith, E. W. Bittner, W. Shi, J. K. Johnson, B. C. Bockrath, *J. Phys. Chem. B* **2003**, *107*, 3752 – 3760.
[13] a) L. Pan, M. B. Sander, X. Huang, J. Li, M. Smith, E. Bittner, B. Bockrath, J. K. Johnson, *J. Am. Chem. Soc.* **2004**, *126*, 1308 – 1309; b) D. N. Dybtsev, H. Chun, S. H. Yoon, D. Kim, K. Kim, *J. Am. Chem. Soc.* **2004**, *126*, 32 – 33; c) G. Férey, M. Latroche, C. Serre, F. Millange, T. Loiseau, A. Percheron-Guégan, *Chem. Commun.* **2003**, 2976 – 2977.

